EXPERIMENTAL CHARACTERIZATION OF THE MIMO CHANNEL TEMPORAL BEHAVIOR

M. A. Jensen*, **J. W. Wallace**†

*Department of Electrical and Computer Engineering, Brigham Young University
Provo, UT 84602, USA, jensen@ee.byu.edu

†School of Engineering and Science, Jacobs University Bremen
28725 Bremen, Germany, wall@ieee.org

Keywords: MIMO systems, Time-varying channels, Information theory

Abstract

This paper analyzes temporal variation in measured multiple-input multiple-output (MIMO) wireless channels with moving communication nodes. A wideband 8×8 sounder is employed to measure the response of indoor and outdoor channels at 2.55 and 5.2 GHz. The rate of channel temporal variation is then quantified in terms of information theoretic metrics that indicate the loss in channel quality as transmit and receive channel state information becomes increasingly outdated.

1 Introduction

Numerous different analytical and experimental studies have revealed the dramatic capacity increase enabled by exploiting the multipath spatial structure with multiple-input multiple-output (MIMO) communications [5]. However, realization of this benefit depends critically on the availability of channel state information (CSI) [3] typically obtained by periodic transmission of known training sequences. When the channel varies rapidly, such as might occur when one or both of the communication nodes is moving, the required training frequency can reduce and eventually eliminate the capacity improvement enabled by MIMO technology.

Because the degree of channel time variation limits the achievable MIMO performance, it becomes essential that we obtain an understanding of the channel temporal properties. While there has been some preliminary work on MIMO channel time variation [2, 7, 11, 13], fully understanding the implications of this phenomenon requires formulation of a comprehensive analysis which applies rigorous metrics for MIMO channel variation to real-world channel measurements.

This paper reveals the results of measurements taken at 2.5 and 5.2 GHz in several representative indoor and outdoor environments. Simple analysis of the channel eigenmodes reveals the extent of the time variation due to node motion. Furthermore, information theoretic metrics which approximate the loss in capacity due to outdated CSI and the receiver and/or the transmitter are formulated and applied to the data in order to quantify the full impact of the channel temporal variation on practical system performance. The results reveal that in most cases, transmit CSI remains useful for several wavelengths, due likely to the fact that the important role of the transmitter is to direct energy into the proper spatial directions. In contrast, receive CSI must be updated approximately every tenth of a wavelength in order to maintain reasonable performance.

2 Channel Measurements

2.1 Measurement System

Figure 1 shows a block diagram of the wideband 8×8 MIMO channel sounder used for the measurements in this campaign [8–10]. The system uses an arbitrary waveform generator to create a multi-tone signal with up to 100 MHz of instantaneous bandwidth. This signal is then up-converted to an RF carrier, amplified, and fed to a microwave switch which routes the signal to one of eight transmit antennas. For the measurements in this work, the transmit antenna is a uniform circular array (UCA) of eight monopoles ($\lambda/2$ inter-element spacing). Each transmit element has its own power amplifier to avoid transmit power limitations imposed by the switch specifications.

At the receiver, a microwave switch routes signals from the eight-element monopole UCA to a receiver which performs low noise amplification, down-conversion, automatic gain control (AGC), and A/D conversion on a personal computer (PC). Microwave switch control is performed by a custom-designed synchronization unit that scans all possible antenna combinations, where the number of antennas and dwell time are selectable. Highly stable 10 MHz rubidium time/frequency references provide transmit/receive system synchronization. The receive waveforms and AGC levels are stored on the PC for channel coefficient estimation.

2.2 Indoor Measurements

For indoor environments, the transmit signal consists of eight tones with 10 MHz separation at a center frequency of either 2.55 or 5.2 GHz and an average transmit power of 200 mW. The system uses a dwell time of 50 μs on each antenna either every

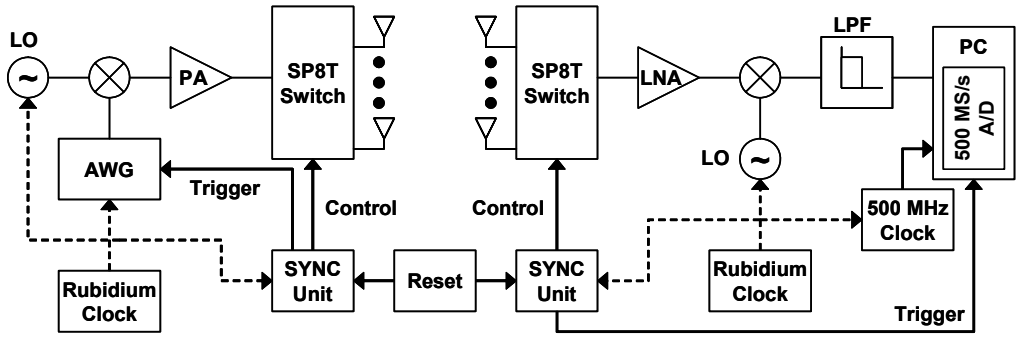

Figure 1: Block diagram of the 8×8 wideband MIMO channel sounder used for the measurements reported in this work.

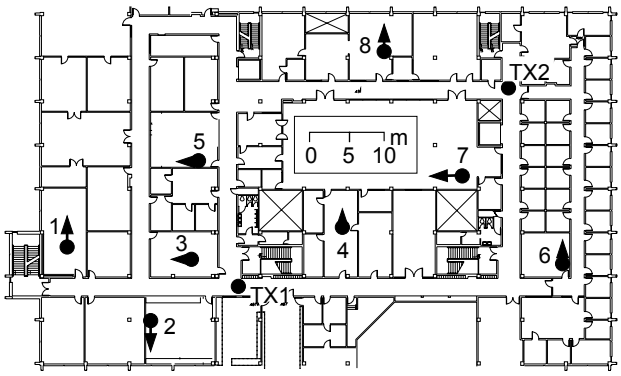

Figure 2: Indoor measurement scenario, where each number indicates a receive location. TX 1 and 2 are the transmit locations for receive Locations 1-5 and 6-8, respectively. Circles and arrows indicate starting RX position and distance/direction moved, respectively.

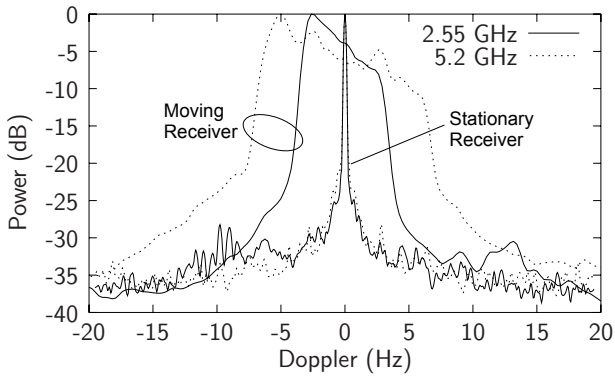

Figure 3: Average Doppler spectrum for indoor measurements for Locations 1-8 for stationary and moving measurements at 2.55 and 5.2 GHz

3.2 ms (fast mode, 1.875 s acquisition time) or every 25.6 ms (slow mode, 15 s acquisition time).

Figure 2 shows a floor plan of the indoor environment along with the locations of the measurements. The transmitter was located at two different hallway positions (held stationary), while the receiver was moved at 30 cm/s along the eight different paths indicated. The cart speed was controlled by coordinating the cart position relative to marks on the floor and timing sounds generated by the computer, with a resulting speed error of approximately ± 1 cm/s.

In each room, tests were performed with the transmitter off and receiver stationary to ensure that the level of co-channel interference was negligible. The subsequent measurements were then taken with either a stationary or moving (fast acquisition mode) receiver. Figure 3 plots the resulting Doppler spectrum averaged over all eight indoor locations, with the 1 Hz maximum Doppler for stationary measurements being small compared to the 5-10 Hz maximum Doppler for moving measurements. These results reveal that the effects of moving scatterers in the environment are relatively unimportant and that even slow acquisition meets the Nyquist criterion for capturing the channel time variation.

2.3 Outdoor Measurements

Because the outdoor measurements involved longer ranges and more difficult propagation environments, achieving adequate signal-to-noise ratio (SNR) at the receiver required a significantly larger transmit power spectral density. Therefore, the transmit signal used 8 MHz of bandwidth (eight tones with 1 MHz spacing) as opposed to the 80 MHz of bandwidth used for the indoor scenarios. Because of the lower transmission bandwidth, fast 3.2 ms acquisition could be performed for a complete 15 s. All measurements were performed at 2.55 GHz center frequency and an average transmit power of 2 W.

Figure 4 provides a map of the outdoor scenario consisting of classroom buildings (C) with brick and cinder block construction, temporary (T) metal structures, and a heating plant (P). Many stationary cars are parked along the street. The transmitter was placed at a single position while the receiver was placed at nine different positions on the street or sidewalks as shown. Figure 5 plots the average Doppler spectrum for measurements with the receiver stationary or moving at 30 cm/s, with respective maximum Dopplers of about 1 Hz and 5 Hz. Here again, the effect of moving scatterers appears to be small.

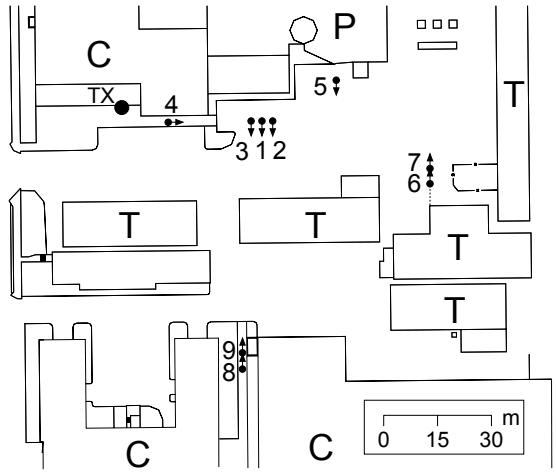

Figure 4: Outdoor measurement scenario consisting of classroom buildings (C), temporary metal structures (T) and a heating plant (P), where numbers indicate a receive location and TX the transmit location. Circles and arrows indicate starting RX position and distance/direction moved, respectively.

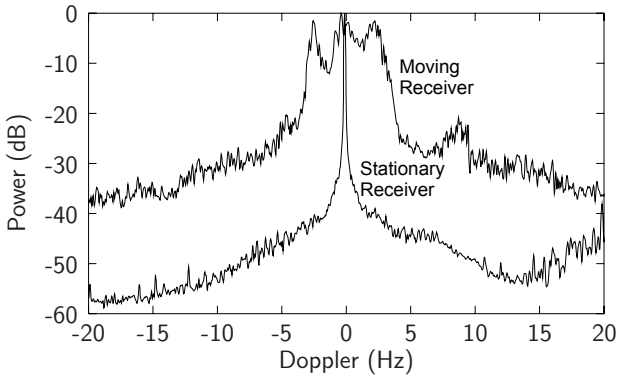

Figure 5: Average Doppler spectrum for outdoor measurements with a stationary and moving receiver at 2.55 GHz

3 MIMO Time-variation Metrics

Quantification of the time-variation of the measured channels requires development of appropriate metrics for MIMO systems. Although these metrics are intended for *time*-varying channels, we characterize variation versus movement *distance*, allowing the results to be scaled according to speed.

Consider the narrowband MIMO system described by

$$\mathbf{y} = \mathbf{H}\mathbf{x} + \boldsymbol{\eta}, \tag{1}$$

where $\mathbf{x}$ is the vector of input signals, $\mathbf{H}$ is the channel transfer matrix, $\boldsymbol{\eta}$ is the vector of receiver noise samples, and $\mathbf{y}$ is the vector of receive signals. Since this work emphasizes the channel evolution, we assume that the initial estimate $\hat{\mathbf{H}}$ of the channel transfer matrix at zero displacement is error free.

We define capacity as a function of displacement d as the instantaneous mutual information given knowledge of the channel at $d = 0$. As d increases, we expect a capacity reduction as the CSI becomes increasingly outdated. Such a capacity degradation metric is related to capacity under imperfect CSI where the initial channel estimate $\hat{\mathbf{H}}$ is in error [6, 12]. The unique goal of this work, however, is to infer from MIMO measurements the elapsed time (or distance moved) beyond which an initial channel estimate is no longer suitable for high-capacity communications, information which is useful to the system designer who must choose transmit/receive CSI update rates and system adaptation strategies. We note that capacity degradation with outdated receive CSI has been studied by other researchers resulting in the development of similar metrics [1, 7, 11].

3.1 Transmit CSI Delay (TCD)

First, consider the case of *transmit CSI delay* (TCD) where the receiver has perfect CSI ($\mathbf{H}$) but the transmitter only has the delayed channel estimate ($\hat{\mathbf{H}}$). We define capacity for delayed transmit CSI as

$$C_T(\mathbf{H}, \hat{\mathbf{H}}) = \log_2 \left| \frac{\mathbf{H}\mathbf{Q}(\hat{\mathbf{H}})\mathbf{H}^H}{\sigma^2} + \mathbf{I} \right|, \tag{2}$$

where $\mathbf{H}$ is the true channel, σ^2 is the receiver noise variance, $\mathbf{Q}(\hat{\mathbf{H}})$ is the optimal transmit covariance given by the water-filling solution (assuming $\mathbf{H} = \hat{\mathbf{H}}$), $\mathbf{I}$ is the identity matrix, $\mathrm{Tr}\{\mathbf{Q}\} \leq P_T$, $|\cdot|$ is a matrix determinant, and P_T is the total allowed transmit power. In this work, P_T and σ^2 are chosen so that the single-input single-output (SISO) SNR averaged over all channel snapshots at a specific location is 10 dB. As the estimate $\hat{\mathbf{H}}$ becomes increasingly outdated, C_T will tend to decrease. The distance at which the TCD capacity drops below the uninformed transmit capacity (C_T with $\mathbf{Q} = \mathbf{I}$) will be denoted as d_T.

3.2 Receive CSI Delay (RCD)

Next, consider the case of *receive CSI delay* (RCD), where both the transmitter and receiver have outdated CSI. If the transmitter and receiver attempt to form parallel Gaussian channels using the singular value decomposition (SVD) of the delayed channel estimate ($\hat{\mathbf{H}} = \hat{\mathbf{U}}\hat{\mathbf{S}}\hat{\mathbf{V}}^H$), we have

$$\mathbf{y} = \hat{\mathbf{H}}\mathbf{x} + (\mathbf{H} - \hat{\mathbf{H}})\mathbf{x} + \boldsymbol{\eta} \tag{3}$$

$$\underbrace{\hat{\mathbf{U}}^H\mathbf{y}}_{\mathbf{y}'} = \hat{\mathbf{S}}\,\underbrace{(\hat{\mathbf{V}}^H\mathbf{x})}_{\mathbf{x}'} + \underbrace{\hat{\mathbf{U}}^H(\mathbf{H} - \hat{\mathbf{H}})\hat{\mathbf{V}}}_{\mathbf{M}}(\hat{\mathbf{V}}^H\mathbf{x}) + \underbrace{\hat{\mathbf{U}}\boldsymbol{\eta}}_{\boldsymbol{\eta}'}. \tag{4}$$

The approach constructs parallel channels with gains $\hat{S}_{ii}$ but creates self-interference controlled by the matrix $\mathbf{M}$.

For the RCD capacity to be completely general, no arbitrary constraints are placed on the time-variant behavior of $\mathbf{H}$ which leads to unknown statistics for $\mathbf{M}$. Therefore, the signaling strategy cannot be adapted to mitigate the effects of the self-interference. Since defining the capacity of this channel rigorously is difficult, we instead lower bound the capacity by computing the mutual information of a simplified system.

First, we assume that the transmitter uses the signaling strategy that is optimal for the case of no self-interference, or that $\mathbf{x}'$

has zero-mean independent Gaussian elements with covariance $\mathbf{R}_x = \mathrm{E}\{\mathbf{x}'\mathbf{x}'^H\} = \mathrm{diag}(\mathbf{p})$, where p_i is the transmit power allocated to the ith parallel channel. While the statistics of the self-interference term $\mathbf{z} = \mathbf{M}\mathbf{x}'$ are unknown, we make the analysis tractable and lower bound the capacity by assuming they are Gaussian. For a fixed transmit covariance $\mathbf{R}_x$, this leads to the mutual information

$$C'_R(\mathbf{H}, \hat{\mathbf{H}}) = \log_2 |\hat{\mathbf{H}}\mathbf{R}_x\hat{\mathbf{H}}^H(\mathbf{R}_z + \mathbf{I}\sigma^2)^{-1} + \mathbf{I}|, \quad (5)$$

where $\mathbf{R}_z = \mathrm{E}\{\mathbf{z}\mathbf{z}^H\}$. Achieving this mutual information requires the receiver to know the covariance $\mathbf{R}_z$ which implies additional training. However, this contradicts our assumption that the receiver only has knowledge of $\hat{\mathbf{H}}$ at $d = 0$.

A more realistic assumption is that the receiver knows the level of self-interference on the parallel sub-channels but is unaware of the cross-correlation. Then $\mathbf{R}_z$ is assumed to be diagonal with entries $\{\mathbf{R}_z\}_{ii} = \{\mathbf{M}\mathbf{R}_x\mathbf{M}^H\}_{ii}$. For a fixed transmit covariance, the mutual information reduces to

$$C_R(\mathbf{H}, \hat{\mathbf{H}}) = \sum_i \log_2(1 + p_i\hat{S}_{ii}^2/q_i), \quad (6)$$

$$q_i = \{\mathbf{M}\mathbf{R}_x\mathbf{M}^H\}_{ii} + \sigma^2, \quad (7)$$

$$\mathbf{M} = \hat{\mathbf{U}}^H\mathbf{H}\hat{\mathbf{V}} - \mathbf{\Phi}\hat{\mathbf{S}}, \quad (8)$$

where p_i are found according to water-filling (assuming $\mathbf{H} = \hat{\mathbf{H}}$ and $q_i = \sigma^2$), $\mathbf{p} = \mathrm{diag}(\mathbf{R}_x)$, and $\mathbf{\Phi}$ is a diagonal matrix with $|\Phi_{ii}| = 1$. We define d_R as the distance at which C_R drops to 50% of its maximum value.

When $\mathbf{\Phi} = \mathbf{I}$, the definitions for $\mathbf{M}$ in (4) and (8) are identical ($\hat{\mathbf{H}} = \hat{\mathbf{U}}\hat{\mathbf{S}}\hat{\mathbf{V}}^H$), and $\mathbf{M}$ therefore includes the effect of changing phase on the parallel communication channels. However, channel phase variation is uninteresting from the standpoint of time-varying multipath structure since it can arise from system considerations (local oscillator drift, temperature variations), and its impact can be removed by using differential modulation. Therefore, setting $\arg(\Phi_{ii}) = \arg(\{\hat{\mathbf{U}}^H\mathbf{H}\hat{\mathbf{V}}\}_{ii})$ will remove the impact of phase variation of the individual parallel channels and emphasize the impact of the changing channel spatial structure.

The mutual information expression in (6) does not represent actual capacity for a number of reasons. Obviously, the assumptions of independent Gaussian interference will not be true in general. Also, we have neglected the possibility that transmitter and receiver work together to learn the statistical nature of the time-varying channel and adapt their signaling strategy to minimize the self-interference. Although we have investigated this possibility, in practice the capacity gains for such a strategy are usually only modest. Finally, the definition of capacity requires an infinite-time coding window over which channel statistics are stationary, which will clearly not be the case for the arbitrary fading channels we consider. Despite these shortcomings, we feel that the definition is useful as a numerical measure of the level of time variability of MIMO channels in an information theoretic sense.

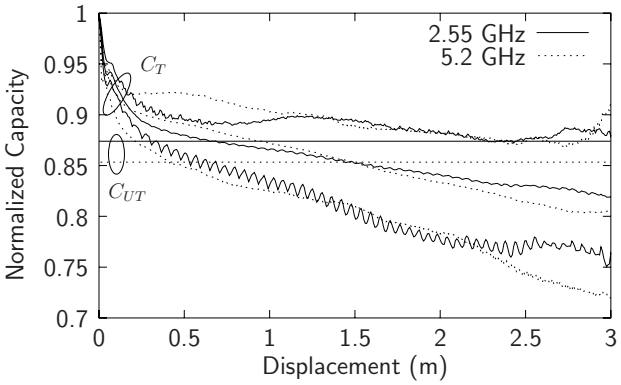

Figure 6: Normalized capacity with delayed transmit CSI (C_T) for indoor Locations 1-8, with curves for maximum, minimum, and mean values at each frequency. The average absolute capacities are 17.7 and 16.6 bits/s/Hz at 2.55 and 5.2 GHz, respectively.

3.3 Averaging

To allow observation of the average channel time-variation behavior, we compute average capacities as

$$C_{T,R}(md) = \frac{1}{M}\sum_{k=1}^{N_F}\sum_{n=1}^{N-m} C_{T,R}(\mathbf{H}^{(k,n+m)}, \mathbf{H}^{(k,n)}), \quad (9)$$

where $\mathbf{H}^{(k,n)}$ is the channel transfer matrix for frequency bin k and distance index n, d is the separation distance of samples, $M = N_F(N-m)$, and N_F and N are the number of frequency bins and distance samples, respectively.

4 Results

In this section, we analyze the TCD and RCD capacity metrics for MIMO channels measured in the indoor and outdoor scenarios described in Section 2.

4.1 Indoor Channels

Figure 6 plots the TCD capacity metric C_T normalized by the maximum value (zero displacement) as a function of distance for the two frequencies. The three sets of curves correspond to the average, maximum, and minimum values over all 8 locations and all frequencies. The displacement is represented as physical distance (m) as opposed to electrical distance (wavelengths) since this scale leads to high agreement between the curves at the two frequencies. This fact suggests that capacity loss due to delayed transmit CSI arises mainly from long-term changes in the multipath structure (direction and power) and not the small-scale fading. The distance d_T at which the capacity curve intersects the uninformed transmit capacity (C_{UT}) represents the distance beyond which transmit CSI is no longer useful.

It is noteworthy that $d_T \approx 0.6$ m and 1.5 m for the 2.55 and 5.2 GHz measurements, respectively. These relatively large values suggest that even infrequent training can benefit performance, somewhat in contrast to conventional wisdom that

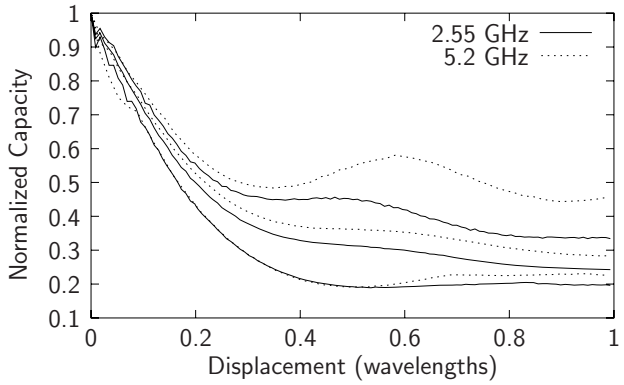

Figure 7: Normalized capacity with delayed receive CSI for indoor Locations 1-8, with curves for maximum, minimum, and mean values at each frequency.

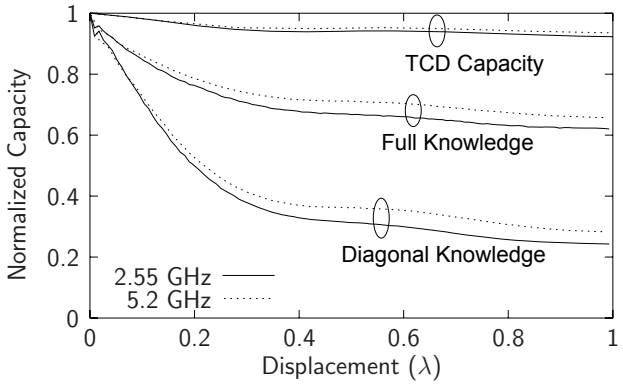

Figure 8: Effect of the knowledge of the self-interference on capacity width delayed receive CSI for indoor Locations 1-8

transmit CSI is impractical due to the required feedback. This observation is similar to that made in [4], where transmit precoding was shown to be beneficial for CSI delays induced by movement of up to about 1.5 m at 2.45 GHz.

Figure 7 plots the normalized RCD capacity as a function of electrical distance at the two frequencies. The similarity of the curves for the two frequencies versus electrical distance suggests that fading controls RCD capacity. The rapid decay in C_R with distance ($d_R \approx \lambda/4$) indicates that training is required frequently (every $\lambda/10$) to maintain high capacity.

The difference in distances over which the transmit and receive CSI is useful stems from the fact that the transmitter need only ensure that the signals are sent in proper directions for achieving good receiver signal quality. As this depends on the multipath spatial structure (angles/gains of departure), this typically varies slowly with distance. The receiver, however, must be able to invert the channel matrix to extract the parallel data streams, a task which requires accurate CSI.

Figure 8 plots the mean capacity for indoor Locations 1-8 assuming knowledge of either all elements or the diagonal elements of $\mathbf{R}_z$, given by expressions (5) and (6), respectively. TCD capacity (perfect knowledge of $\mathbf{M}$ at the receiver) is also plotted for comparison. The results indicate that about half of the capacity loss arises from ignorance of the cross-correlation terms, implying that using additional training to track $\mathbf{R}_z$ could improve performance. If $\mathbf{R}_z$ is slowly varying, such tracking should require modest training requirements. However, this is beyond the scope of this paper and the case of full knowledge of $\mathbf{R}_z$ will not be considered further.

4.2 Outdoor Channels

Figure 9 illustrates the TCD metric for measured outdoor channels at 2.55 GHz, where again average, maximum, and minimum values are included. The average indoor TCD metric at 2.55 GHz as well as the average outdoor uninformed transmit capacity are also shown. Comparison of the data reveals that the long term decay of the outdoor TCD capacity is much slower than that of the indoor value, with $d_T > 3$ m on average.

Figure 10 plots the RCD capacity as a function of electrical distance for outdoor Locations 1-9 along with the average indoor RCD capacity. Interestingly, the outdoor d_R value for the average curve is only slightly longer than that for the indoor measurements. This similarity is remarkable, since the two channels should have very different scattering characteristics, further suggesting that RCD capacity reduction is somewhat insensitive to the exact multipath structure.

5 Conclusion

Although MIMO systems exhibit high capacity with perfect CSI, imperfect CSI can lead to reductions in available capacity. This paper had explored the effect of temporal variations on measured indoor and outdoor MIMO channels with receiver movement. Two metrics were developed that quantify the loss in channel quality in an information theoretic sense as either transmit or receive CSI becomes increasingly outdated. These metrics applied to indoor and outdoor 8×8 MIMO measurements at 2.55 and 5.2 GHz indicated that although transmit CSI can be useful for 10s of wavelengths, receive CSI must be updated on the order of $\lambda/10$ for high channel capacity.

References

[1] J. Du, Y. Li, D. Gu, A. F. Molisch, and J. Zhang, "Estimation of performance loss due to delay in channel feedback in MIMO systems," in *Proc. 2004 IEEE 60th Veh. Technol. Conf.*, (Los Angeles, CA), pp. 1619–1622, 26-29 Sep. 2004.

[2] G. D. Galdo, M. Haardt, and M. Milojevic, "A subspace-based channel model for frequency selective time variant MIMO channels," in *Proc. 2004 IEEE 15th Intl. Symp. on Personal, Indoor and Mobile Radio Comm.*, vol. 3, (Barcelona, Spain), pp. 1603–1607, Sep. 5-8 2004.

[3] A. Goldsmith, S. A. Jafar, N. Jindal, and S. Vishwanath, "Capacity limits of MIMO channels," *IEEE Trans. Inf. Theory*, vol. 21, pp. 684–702, Jun. 2003.

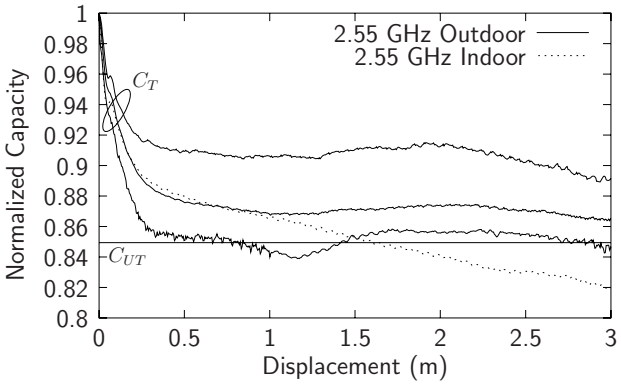

Figure 9: Normalized capacity with delayed transmit CSI for outdoor Locations 1-9, with curves for maximum, minimum, and mean values at 2.55 GHz. Also plotted are the average uninformed transmit capacity for the outdoor cases and the mean TCD capacity for indoor locations.

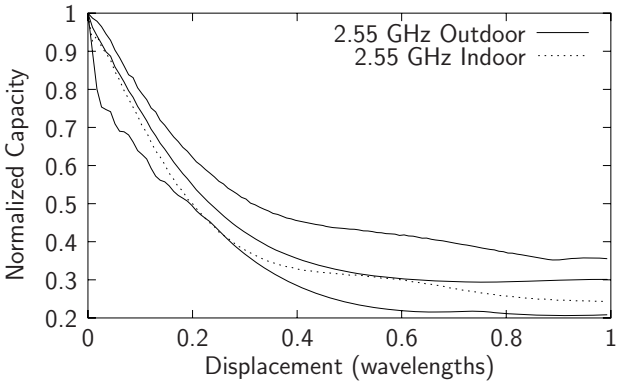

Figure 10: Normalized capacity with delayed receive CSI for outdoor Locations 1-9, with curves for maximum, minimum, and mean values at 2.55 GHz. Also plotted is the mean RCD capacity for indoor locations.

[4] M. Herdin, N. Czink, H. Ozcelik, and E. Bonek, "Correlation matrix distance, a meaningful measure for evaluation of non-stationary MIMO channels," in *Proc. 2005 IEEE 61st Veh. Technol. Conf.*, vol. 1, (Stockholm, Sweden), pp. 136–140, 30 May-1 Jun. 2005.

[5] M. A. Jensen and J. W. Wallace, "A review of antennas and propagation for MIMO wireless communications," *IEEE Trans. Antennas Propag.*, pp. 2810–2824, Nov. 2004.

[6] P. Kyritsi, R. A. Valenzuela, and D. C. Cox, "Channel and capacity estimation errors," *IEEE Commun. Lett.*, vol. 6, pp. 517–519, Dec. 2002.

[7] J. Maurer, C. Waldschmidt, T. Kayser, and W. Wiesbeck, "Characterisation of the time-dependent urban MIMO channel in FDD communication systems," in *Proc. 2003 IEEE 57th Veh. Technol. Conf.*, vol. 4, (Seoul, Korea), pp. 544–548, Apr. 22-25 2003.

[8] B. T. Maharaj, L. P. Linde, J. W. Wallace, and M. Jensen, "A cost-effective wideband MIMO channel sounder and initial co-located 2.4 GHz and 5.2 GHz measurements," in *Proc. 2005 IEEE Intl. Conf. Acoustics, Speech, and Signal Processing*, vol. 3, (Philadelphia, PA), pp. 981–984, Mar. 18-23 2005.

[9] B. T. Maharaj, J. W. Wallace, and M. A. Jensen, "Experimental evaluation of the MIMO wideband channel temporal variation," in *Proc. 2005 URSI 28th General Assembly*, (Delhi, India), Oct. 23-29 2005.

[10] B. T. Maharaj, J. W. Wallace, L. P. Linde, and M. A. Jensen, "Linear dependence of double-directional spatial power spectra at 2.4 and 5.2 GHz from indoor MIMO channel measurements," *Electronics Letters*, vol. 41, pp. 1338–1340, 24 Nov. 2005.

[11] V. Pohl, P. H. Nguyen, V. Jungnickel, and C. von Helmolt, "Continuous flat-fading MIMO channels: achievable rate and optimal length of the training and data phases," *IEEE Trans. Wireless Commun.*, vol. 4, pp. 1889–1900, July 2005.

[12] T. Yoo and A. Goldsmith, "Capacity of fading MIMO channels with channel estimation error," in *Proc. 2004 IEEE Intl. Conf. Commun.*, vol. 2, (Paris, France), pp. 808–813, Jun. 20-24 2004.

[13] T. Zwick, C. Fischer, and W. Wiesbeck, "A stochastic multipath channel model including path directions for indoor environments," *IEEE J. Selected Areas Commun.*, vol. 20, pp. 1178–1192, Aug. 2002.